Enhancing the Mechanical Properties of Glassy Nanocomposites by Tuning Polymer Molecular Weight

Anne-Caroline Genix, Vera Bocharova, Alexander Kisliuk, Bobby Carroll, Sheng Zhao, Julian Oberdisse, Alexei P. Sokolov

Enhancing Mechanical Properties of Glassy Nanocomposites by Tuning Polymer Molecular Weight

Anne-Caroline Genix,[1*] Vera Bocharova,[2*] Alexander Kisliuk,[2] Bobby Carroll,[2] Sheng Zhao,[3] Julian Oberdisse [1] and Alexei P. Sokolov [2,3]

[1] *Laboratoire Charles Coulomb (L2C), Université de Montpellier, CNRS, F-34095 Montpellier, France*

[2] *Chemical Sciences Division, Oak Ridge National Laboratory, Oak Ridge, TN 37831, USA*

[3] *Department of Chemistry, University of Tennessee, Knoxville, TN 37996, USA*

Corresponding Authors

*E-mail: anne-caroline.genix@umontpellier.fr

*E-mail: bocharovav@ornl.gov

KEYWORDS: Polymer nanocomposites, mechanical reinforcement, glass transition, segmental dynamics, interfacial layer

ABSTRACT

The addition of nanoparticles to a polymer matrix is a well-known process to improve mechanical properties of polymers. Many studies of the mechanical reinforcement in polymer nanocomposites (PNCs) focus on rubbery matrices; however, much less effort concentrates on factors controlling mechanical performance of the technologically important glassy PNCs. This paper presents a study of the effect of the polymer molecular weight (MW) on the overall mechanical properties of glassy PNCs with attractive interaction by using Brillouin light scattering. We found that the mechanical moduli (bulk and shear) have a non-monotonic dependence on MW that cannot be predicted by simple rule of mixtures. The moduli increase with increasing MW up to 100 kg/mol followed by a drop at higher MW. We demonstrate that the change in the mechanical properties of PNCs can be associated with the properties of the interfacial polymer layer. The latter depend on the interfacial chain packing and stretching, as well as polymer bridging that vary differently with MW of the polymer. These competing contributions lead to the observed non-monotonic variations of glassy PNC moduli with MW. Our work provides a simple, cost-effective, and efficient way to control the mechanical properties of glassy PNCs by tuning the polymer chain length. Our finding can be beneficial for rational design of PNCs with desired mechanical performance.

Polymer nanocomposites (PNCs) have become a prominent area of current research and development. Addition of hard nanoparticles to a polymer matrix leads to a significant improvement of several macroscopic properties, such as electrical [1] or mechanical properties, [2-3] as well as reduction in membrane aging. [4] This makes PNCs attractive for various applications, including surface coating, electronics, and gas separation membranes. In industry, combinatory methods are often used to design PNCs. These methods do not always lead to the desired properties, highlighting the importance of a fundamental understanding of the factors affecting macroscopic properties in PNCs. Our fundamental knowledge is rather limited with many open questions, and especially those related to the microscopic origin of the mechanical reinforcement found for PNCs in rubbery and in glassy states.[5-10] Several mechanisms, such as particle jamming [11] and the formation of bridges between NPs,[8-9] have been proposed to explain the increase in the mechanical moduli in rubbery nanocomposites. However, much less is known about mechanical enhancement in glassy PNCs due to the range of non-equilibrium states available for polymers, and the limited number of experimental techniques to study viscoelastic, dynamic, and mechanical properties of glassy polymers. Although the mechanical enhancement in a glassy PNC is large in absolute values (a few GPa increase in modulus), the changes relative to the neat glassy polymer are usually small (a few times),[10, 12-14] and difficult to measure. Originally, the mechanical enhancement in the glassy PNCs is interpreted by the hydrodynamic effect of the hard nanoparticles. [15] This effect is due to the deformation of the flow field around the particle. It has been shown by Smallwood [16] and Guth [17] that the force field on the polymer surrounding the particle can be mapped on the flow field, leading to the same relative increase in modulus as given by Einstein [18] for viscosity, i.e., $1 + 2.5\,\Phi$ at low volume fractions Φ. However, recent mechanical tests on glassy PNCs have clearly shown that mechanical reinforcement is stronger than predicted

by the hydrodynamic approach. [10] Besides, the dispersion state, i.e., the spatial arrangements of the nanoparticles (NPs) within the matrix, has a strong impact on the mechanical performances. Whereas the formation of a volume-spanning network of NPs, or NP aggregates might have advantages in the melt state, [19-23] well-dispersed NPs are required to obtain optimal mechanical properties below the glass-transition temperature, T_g. [12, 24-25] This indicates that different mechanisms contribute to the reinforcement in glassy and rubbery PNCs.

Recently, the concept of an interfacial polymer layer with a thickness of ~ 2 – 6 nm around the nanoparticles and enhanced moduli has been employed to explain the mechanical properties of PNCs in both the rubbery and glassy states. [9-10, 26] For rubbery PNCs, a spatial dependence of the viscoelastic modulus of the polymer chains has been proposed in relationship with the concept of T_g-gradient. [7, 27] In this approach, it is expected that the interfacial layer modulus will be about 10^2 – 10^3 times higher than that of the bulk rubbery polymer. This increase occurs because the adsorbed polymer layer surrounding the nanoparticles displays an increased T_g in the case of attractive polymer-filler interaction, and it might be in a glassy state even when the polymer matrix is still in a rubbery state (above T_g). This leads to a higher mechanical moduli (glassy) with respect to the neat polymer (rubbery moduli). Enhancement of the interfacial layer modulus has later been confirmed via a direct nanoscale probing of the mechanical properties of the layer with atomic force microscopy (AFM), where an increase of approximately one order of magnitude was found with respect to the neat rubbery polymer. [28] In glassy PNCs, AFM measurements have also indicated the presence of an interfacial layer with higher modulus than the neat polymer, [10, 29] in agreement with recent nanoindentation simulations [30]. However, the data on the magnitude of the elastic response as well as the extent of the interphase are usually very scattered, [30-31] which make

quantitative determinations of the local interfacial layer properties a challenging task when using AFM. Therefore, other methods capable of investigating the mechanical properties at the interface are required in glassy PNCs.

Brillouin light scattering (BLS) is a non-destructive optical technique based on the inelastic scattering of visible light by thermal acoustic phonons, which can be used in both glassy and rubbery PNCs. [32] It allows accessing the velocity of sound in the system and therefore the elastic properties (longitudinal and shear moduli) in the Gigaherz frequency range related to microscopic length scales. Note that dynamic mechanical analysis or tensile tests provide macroscopic properties, and are more sensitive to secondary relaxations, sample quality, and defects. Several BLS studies have provided evidence of mechanical reinforcement in glassy PNCs. [10, 32-34] It was found that both the shear and bulk moduli increase with particle loading, and that this increase cannot be explained by a two-phase model [35] assuming NPs dispersed in a homogeneous matrix. [10, 26] This discrepancy is a clear indication of an additional mechanism for reinforcement other than the hydrodynamic effect, and it has been associated with the presence of an interphase with higher modulus in the vicinity of the nanoparticles. The interfacial layer moduli were found to be about 2 times higher than that of the matrix using the interfacial layer model (ILM) [36] approach developed for multi-component systems. On the other hand, other BLS studies have reported opposite evolutions of the PNC elastic properties depending on the process conditions (solvent choice and annealing), [33] or on the NP-polymer interaction using different types of surface modification, like silanization [37] and chain grafting [38-39]. In particular, recently it has been found that a PNC with grafted polymer chains displays lower moduli in the interfacial layer than in the case of PNC filled with bare NPs, while still having a higher T_g and stronger suppression of the segmental dynamics.

[39] Such a counter-intuitive behavior suggests a competition between different effects, namely frustration in chain packing (density) and chain conformation (stretching) in the interfacial layer. These effects can be varied by the polymer grafting density, and a low grafting density resulted in a reduction of density and of the mechanical properties of the grafted PNCs. All these observations highlight the prevalent role played by both the structural organization and dynamics of the interfacial layer. In this context, the chain length or polymer molecular weight (MW) is an important parameter. In PNCs with attractive interactions, both theoretical [40] and experimental [41] studies have suggested that the chains form a physically adsorbed layer at the NP interface with an average thickness proportional to the polymer radius of gyration. Such a bound layer gives rise to a dynamic interfacial layer with different segmental dynamics [26] and also different mechanical properties than the bulk, as discussed above. Whereas one of our recent works report on the unexpected MW-dependence of the interfacial layer thickness, which slightly decreases with increasing chain length, [42] the evolution of elastic properties of the interfacial layer with MW has never been studied to the best of our knowledge. Such studies of microscopic parameters controlling macroscopic mechanical properties in glassy PNCs are highly desirable for both fundamental research and practical applications.

This paper focuses on studies of the polymer molecular weight effect on the mechanical (bulk and shear moduli) and dynamic properties of PNCs in the glassy state. We study a model nanocomposite system based on poly(2-vinylpyridine) (P2VP) with a fixed loading of silica nanoparticles (≈ 40 wt%), by combining Brillouin light scattering (BLS), small-angle X-ray scattering (SAXS), broadband dielectric spectroscopy (BDS), and temperature-modulated differential scanning calorimetry (TMDSC). We deliberately choose a high filler content to

achieve maximum enhancement of mechanical properties, while still maintaining reasonable processability of the film, which is important for practical applications. Our analysis reveals that the chain length has a strong influence on the resulting mechanical reinforcements in PNCs below T_g. PNCs with low MW exhibit a stronger enhancement of mechanical properties compared to the PNCs with high MWs. We ascribe the observed difference in mechanical reinforcement to an increase in chain packing frustration in the interfacial layer with increase in MW. Our results demonstrate that the PNC's mechanical moduli can be effectively tuned by changing only the chain length, and that depending on molecular weight they can be either increased or decreased.

Materials and Methods

Materials. Poly(2-vinylpyridine) with different weight-average molecular weights (MW = 9.1, 35.9, 101.1, 216, and 404 kg/mol and polydispersity index below 1.2) were purchased from Scientific Polymer Products Inc., and used as received. The silica nanoparticles (SiO_2 NPs) were synthesized by a modified Stöber method [43] in ethanol with the final NP concentration of 16 mg/ml. They were characterized by SAXS in ethanol at 0.7 vol% dilution. The scattered intensity revealed a log-normal size distribution (R_0 = 9.7 nm, σ = 17%), leading to an average nanoparticle radius of 9.85 nm.

Preparation of polymer nanocomposites. The polymer and nanoparticles were mixed in ethanol with proportions calculated to obtain a nominal silica content of 26 vol% in the final PNCs. Solvent was evaporated during stirring at room temperature before further drying under vacuum at 403 K for 48 hours in Teflon dishes. The real silica fractions in nanocomposites were obtained by thermogravimetric analysis (TGA, Q50, TA Instruments, 20 K/min, under air) from the weight loss between 403 K and 1073 K. The silica volume fraction, Φ_{NP}, was determined by mass

conservation using the density of the neat polymers measured by pycnometry and the silica density, ρ_{NP} = 2.406 g·cm^{-3}. [10] Differences in the obtained Φ_{NP} with respect to the expected values are due to pipetting errors and precision of the weighting, and do not exceed 5%. The glass-transition temperature, T_g, was determined using temperature-modulated differential scanning calorimetry (Q2000, TA Instruments). Samples of about 10 mg were sealed in aluminum Tzero pans and annealed at 433 K for 20 min. Then, they were measured at an average 2 K/min rate with temperature modulation amplitude and period of ±0.5 K and 60 s, respectively. T_g was defined as the inflexion point temperature in the reversible heat flow upon heating.

Small-angle X-ray scattering (SAXS) experiments were performed with an in-house setup of the Laboratoire Charles Coulomb, "Réseau X et gamma", University of Montpellier, France. A high brightness low power X-ray tube, coupled with aspheric multilayer optics (GeniX^{3D} from Xenocs) was employed. It delivers an ultralow divergent beam (0.5 mrad). Scatterless slits were used to give a clean 0.6 mm beam diameter with a flux of 35 Mphotons/s at the sample. We worked in a transmission configuration and scattered intensity was measured by a 2D "Pilatus" pixel detector, at a distance of 1900 mm from the sample. The scattering of the neat polymers, I_{Neat}, has been measured independently in order to subtract the matrix contribution, $(1-\Phi_{NP})\ I_{Neat}$, for each PNC sample.

Broadband dielectric spectroscopy (BDS). Dielectric spectra were measured using disk-shaped samples with a diameter of 20 mm. All samples have been hot pressed (423 K) to reach a typical thickness of 0.15 mm, prior to drying under vacuum at 393 K for 3 days. Thin films were then placed between gold plated electrodes forming a capacitor. For pure matrices, a ring of Teflon (inner diameter of 16 mm, thickness 0.14 mm) was used as a spacer to prevent possible short-circuits due to polymer flow. A broadband high-resolution dielectric spectrometer (Novocontrol

Alpha) was used to measure the complex dielectric permittivity, $\varepsilon^*(\omega) = \varepsilon'(\omega) - i\,\varepsilon''(\omega)$, in the frequency range from 10^{-2} to 10^7 Hz ($\omega = 2\pi f$). Before measurement each sample was annealed for 1 h at 433 K in the BDS cryostat (under nitrogen atmosphere). Then isothermal frequency measurements have been performed from 433 K down to 103 K, with temperature stability better than 0.1 K. Then, the spectra were measured again at 293 K and 433 K in order to check the reproducibility of our measurements. Accurate estimates of the volume fraction of the interfacial layer require accurate measurements of the dielectric spectra in absolute values. To achieve that, and to get rid of possible artefacts coming from (i) different surface states of the samples and (ii) thickness variation due to temperature change, the complex permittivities have been normalized using spectra measured at the lowest measurable temperature, T = 103 K. The real part of the permittivity at such a low temperature corresponds to the dielectric constant, ε_∞, which relates to the refractive index. Considering that the latter depends on the molecular weight of the polymer only at small values (typically below a few thousand), [44] we used an MW-independent value of ε_∞. In practice, the ε'(103 K) for the neat polymers have been rescaled to 3.05 using measurements on the 36k-matrix. For PNCs, ε_∞ was calculated using a two-component model [45] that included silica volume fraction, as well as taking ε_∞ = 3.05 and 3.9 [42] for the polymer and silica permittivity values, respectively (see SI for details). PNC data at 103 K were rescaled to this theoretical value, and then the permittivity data at all other temperatures were rescaled by the same value estimated at T= 103 K.

Density measurements. All samples were dried in the oven for at least 12 hours at 393 K before density measurement. Density was measured at room temperature on Pycnometer AccuPyc II 1340 in helium. Each sample was measured at least seven times and the average value is presented in Table 1. The standard deviation was found to be on the order of 1%.

Brillouin light scattering (BLS). Bubble-free polymer nanocomposite disks with a diameter of 10 mm and a thickness of 1 mm were first prepared and sandwiched by two sapphire glass windows at 393 K and stored at this temperature in an oven under vacuum. The temperature was then decreased to ambient very slowly using a cooling rate of about 0.2 K/min. All BLS measurements were conducted in a symmetric scattering geometry at a 90 degree scattering angle using a solid state laser (Verdi, λ_{laser} = 532 nm). [39] The power of the incident laser beam was ~ 5 mW. The advantage of the symmetric scattering geometry is the compensation of the refractive index, [46] which provides an estimate of the sound velocity from the Brillouin peak frequency without knowledge of the materials refractive index. Both VV and VH polarizations were utilized to capture the longitudinal (VV and VH) and transverse modes (VH). All the measurements were performed at room temperature with mirror distances in the tandem Fabry-Pérot interferometer fixed to 7 mm for VV and 15 mm for VH polarizations, which covers the frequency range between 2 GHz and 21 GHz with a resolution of 0.04 GHz. The experimental error bar for the longitudinal (V_L) and transverse (V_T) sound velocities did not exceed 0.2%.

Results and Discussion

Table 1 presents the characterization results of neat P2VP and silica-filled P2VP nanocomposites (similar loadings) with different polymer molecular weights from 9 to 404 kg/mol. The T_g of the PNCs is found to increase by ~ 1.5 – 5 K relative to the pure matrices (see SI for an illustration of the trend in T_g and density).

Table 1. Characteristics of P2VP matrices and PNCs: sample name, silica concentration from TGA, glass-transition temperature from TMDSC and BDS, longitudinal (V_L) and transverse (V_T) sound velocities from BLS, bulk (K) and shear (G) moduli.

Sample name	Φ_{NP} [vol%]	T_g (TMDSC) [K]	T_g (BDS) [K]	Density [kg/m^3]	V_L [m/s]	V_T [m/s]	K [GPa]	G [GPa]
Neat-9k	0	364.3	357.9	1129	2652	1355	5.18±0.07	2.07±0.02
Neat-36k	0	373.1	366.1	1194	2616	1325	5.38±0.07	2.10±0.02
Neat-101k	0	376.6	369.3	1211	2606	1325	5.39±0.07	2.12±0.02
Neat-216k	0	377.1	368.5	1222	2608	1330	5.43±0.09	2.16±0.04
Neat-404k	0	376.8	369.2	1224	2605	1328	5.42±0.07	2.16±0.02
PNC-9k	26.3	369.6	365.0	1470	2899	1581	7.46±0.11	3.67±0.03
PNC-36k	25.0	375.5	370.7	1483	2955	1625	7.73±0.12	3.92±0.03
PNC-101k	26.3	378.5	373.1	1513	2943	1630	7.74±0.12	4.02±0.03
PNC-216k	27.3	378.5	372.1	1494	2936	1617	7.67±0.12	3.91±0.03
PNC-404k	26.1	378.2	372.6	1446	2924	1616	7.32±0.11	3.77±0.03

SAXS was used to analyze the nanoparticle dispersion in PNCs, where the scattered intensities were compared to form factor scattering (Figure 1a). All spectra show a well-defined repulsive interaction peak at intermediate q, corresponding to a dominant distance in the nanoparticle dispersion. The observed differences at low q may result from slight differences in the interactions and large-scale distribution of the filler particles in the matrix. It may for instance be caused by impurities. The local structure on the length scale of interest, i.e. the first layers of neighbors between particles as evidenced by the structure factor peak, turns out to be only marginally affected. The position of the peak, q_{NP}, is related to the typical center-to-center interparticle distance, $d = 2\pi/q_{NP}$, from which the average surface-to-surface interparticle spacing can be obtained, $IPS = d - 2R_{NP}$. The IPS values estimated from SAXS are reported in Figure 1b as $2R_g/IPS$, where R_g is the radius of gyration of the chain. They are in agreement with the theoretical estimates for IPS based on either a cubic or random [47] packing of nanoparticles in the sample, and

the NP volume fraction (Table 1). This result clearly indicates that nanoparticles are uniformly distributed in all PNCs studied here. The final organization of the nanoparticles in the PNC is set during the drying process when only part of the solvent has evaporated. [48] This step leads to a strong increase of the matrix viscosity inducing the freezing of the NP dispersion. As previously observed, [49] the choice of the polymer solvent (here ethanol) is crucial as it controls the formation of an adsorbed polymer layer onto the nanoparticles in suspension. Such a bound layer, whose thickness was found to be of the order of the polymer R_g in similar P2VP-silica PNCs, [50] provides steric stabilization and prevents NP agglomeration that would result from opposite forces like depletion attraction. We emphasize that it is not possible to describe the apparent PNC structure factor using only polydisperse hard-spheres interactions, which indicates the existence of additional repulsive long-range interactions between nanoparticles. The latter are most probably of electrostatic origin resulting from the presence of stabilizing charges on the silica surface. [48]

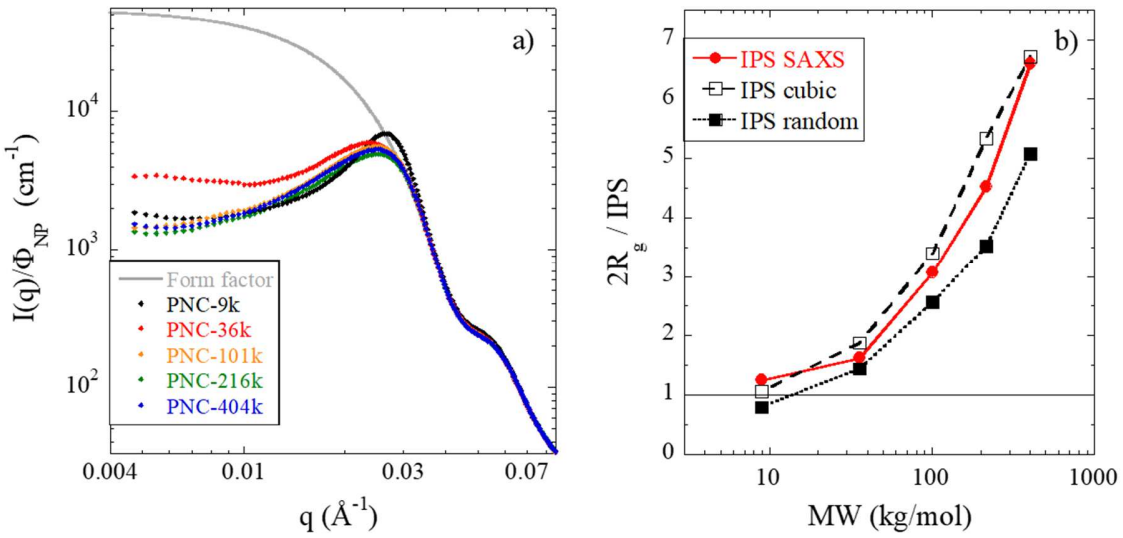

Figure 1. a) Reduced representation of the scattered intensity for a series of P2VP/silica nanocomposites with different molecular weights from 9 to 404 kg/mol and same silica content ($\Phi_{NP} \approx 26$ vol%). The NP form factor normalized to PNC scattering is represented by a continuous line. **b)** Ratio of P2VP chain size ($2R_g$) and different estimations of the interparticle spacing as a function of molecular weight.

Figure 2 presents the BLS spectra with the longitudinal modes (LM) in the main figure, and transverse modes (TM) in the inset, for selected nanocomposites at similar loadings and a pure polymer matrix for comparison. The BLS data of all measured samples (PNCs and neat polymers) are presented in the SI. A clear shift towards high frequency is observed for both the LM and TM of PNCs, indicating a more rigid medium with higher modulus relative to the neat polymer. To extract the longitudinal and transverse sound frequencies, we fit our data to the damped harmonic oscillator model, where we determined frequency of the peak positions ($\nu_{L,T}$). Using the frequencies of the BLS peaks, we estimate the longitudinal and transverse sound velocities (Table 1) using the linear dispersion relationship for acoustic modes: $V_{L,T} = 2\pi\upsilon_{L,T} / Q$, where $Q = 2\pi\sqrt{2} / \lambda_{laser}$ (this equation is valid for symmetric scattering at 90°). The shear ($G = \rho V_T^2$) and longitudinal moduli ($M = \rho V_L^2$) are used to calculate the bulk modulus ($K = M - 4/3G$) by using the mass density measured by pycnometry. [51] The obtained densities and microscopic mechanical moduli for the PNCs and neat polymers are reported in Table 1, and Figure 3a presents the evolution of the PNC moduli K_{PNC} and G_{PNC} with the polymer molecular weight.

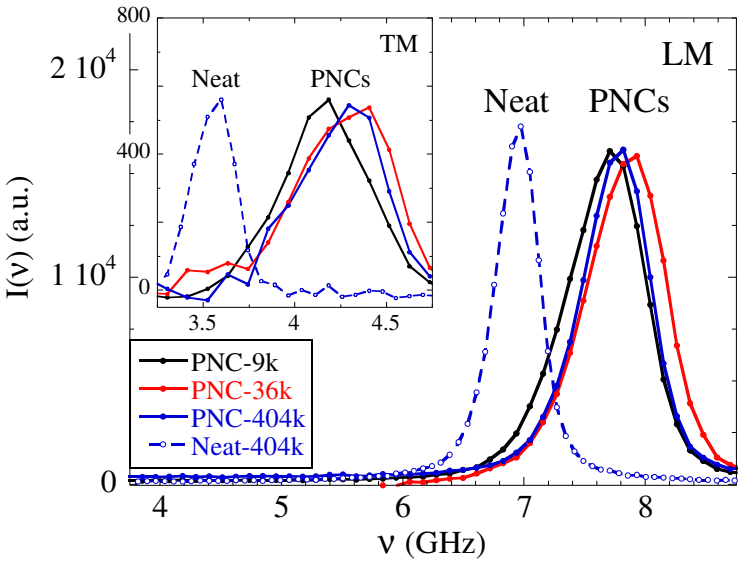

Figure 2. A representative plot of the longitudinal mode (LM) from Brillouin light scattering of neat P2VP (MW = 404 kg/mol) and selected P2VP/silica nanocomposites (PNCs, $\Phi_{NP} \approx 26$ vol%) with MW = 9, 36, and 404 kg/mol. Inset: transverse mode (TM).

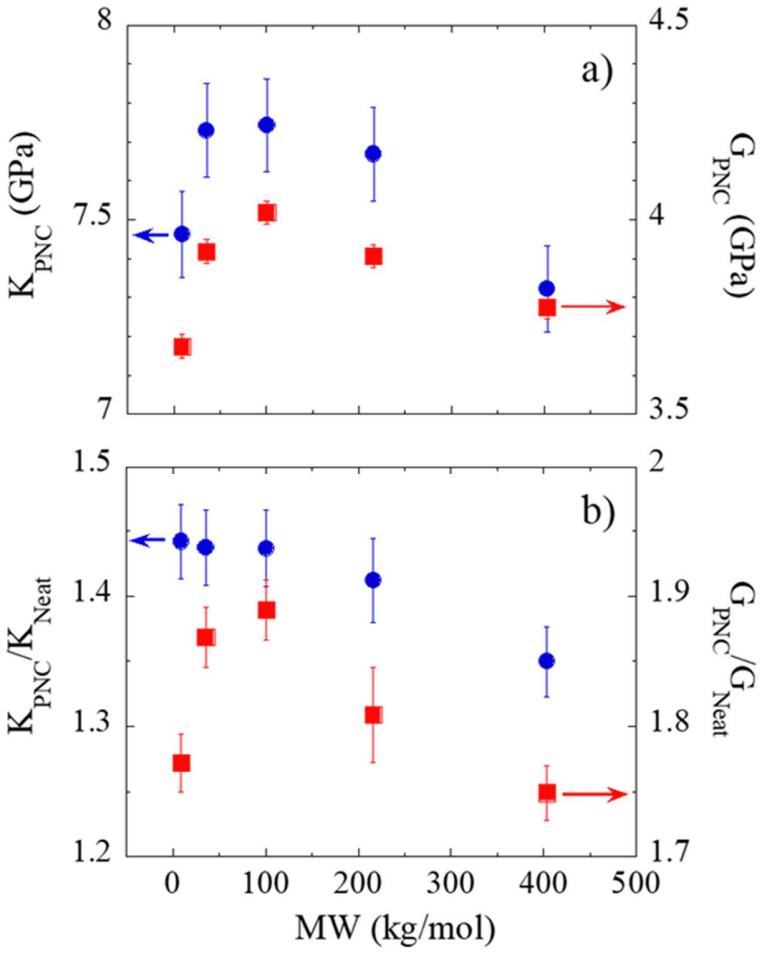

Figure 3. a) Bulk (K) and shear (G) moduli of P2VP/silica nanocomposites with different molecular weights. **b)** Normalization of the PNC moduli on the corresponding moduli of pure polymers with the same MW.

Both PNC moduli exhibit a non-monotonic dependence on MW (Fig. 3): initial increase with MW up to 100 kg/mol, followed by a decrease for higher MWs. To understand these data, we normalized them to the mechanical moduli of the neat polymers (Figure 3b). The non-monotonic trend remains, and it cannot be ascribed to nanoparticle aggregation, which was excluded by the SAXS results. To gain deeper insight into the mechanism of this non-monotonic behavior, a detailed analysis of the mechanical properties in the interfacial polymer layer surrounding the nanoparticles is required. The presence of an interfacial layer caused by the physical adsorption of

the polymer on the NP surface in P2VP-silica nanocomposites has been confirmed in previous studies reported in literature. [39, 52-53] To determine the individual contribution of this layer to the mechanical properties of PNCs, we use the interfacial layer model (ILM) approach developed to describe both mechanical and dielectric properties of heterogeneous systems. [36, 54] Previous BLS studies on P2VP [39] and poly(vinyl acetate) (PVAc) [10] nanocomposites at different silica loadings have demonstrated that ILM provides a much more accurate description of the mechanical properties of PNCs than other existing models. The validity of ILM was also confirmed by a finite element analysis in ref [10]. In order to apply the ILM model to the BLS data, it is first required to determine the volume fraction of the interfacial region, which can be independently obtained using broadband dielectric spectroscopy as detailed in the following part.

Comparisons between the dielectric loss spectra of selected nanocomposites and their corresponding pure matrices are shown in Figure 4. Comparisons for all other MWs are presented in SI. The PNC spectra display a shift of the main relaxation peak associated with the segmental (α-) relaxation towards low frequencies, a reduction of its amplitude, and a significant broadening in the peak shape. The low-frequency broadening of the α-relaxation reveals the interfacial layer contribution, which has slower segmental dynamics than that of the bulk, as previously observed in nanocomposites with attractive polymer-filler interaction. [26, 55-56]

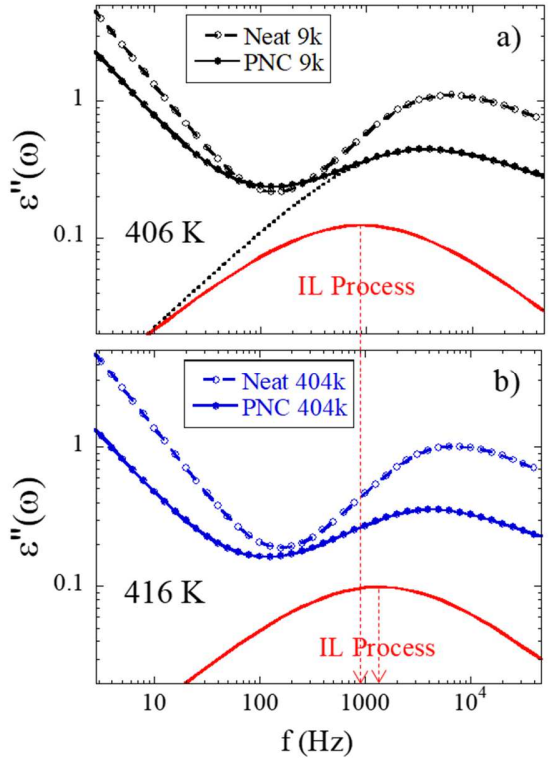

Figure 4. Comparison of the dielectric loss spectra, ε''(ω), of the pure polymer matrix (empty circles) and PNC (plain circles) with MW = 9 kg/mol **(a)** and 404 kg/mol **(b)** both at $1.1T_g$ (T_g of the nanocomposite). The response from the interfacial layer process (red line) is shown for the nanocomposite samples. Arrows indicate the time scale $\tau_{max}=1/(2\pi f_{max})$ of this process. The dotted line for the PNC-9k in (a) presents a fit of the apparent peak maximum by a single HN function.

To describe the dielectric response of the interfacial layer, we use ILM. [54] In this model, we approximate the dielectric function of the interfacial layer by a (symmetric) Cole-Cole function, whereas the polymer bulk contribution was described by a Havriliak−Negami (HN) function [57] having the same spectral shape parameters and time scale as the dielectric function of the neat polymer. We emphasize that the ILM does not simply add these two contributions, but has a more complex form that explicitly takes into account interference terms in the dielectric response of heterogeneous systems (see ref [55] for details). The ILM analysis clearly separates the interfacial layer and bulk-like polymer contributions to the dielectric spectra (see, e.g., data for PNC-9k, and

PNC-404K in Figure 4). This analysis provides estimates of the characteristic relaxation time in the interfacial layer (using the peak position) and the volume fraction of the interfacial layer from the decrease in the amplitude of the bulk-like contribution. Figure 5a presents the temperature dependence of the relaxation times of the interfacial layer in PNCs with two MWs, τ_{IL}, and of the corresponding pure matrices, τ_{neat}. One can see that the interfacial layer process is significantly slower than the dynamics of the bulk polymer and, more importantly, that the amplitude of this slowing down depends on the polymer molecular weight. The evolution of the segmental dynamics of the interfacial layer relative to the bulk, τ_{IL}/τ_{neat}, as a function of molecular weight is shown in the inset of Figure 5a for a selected temperature, T = 1.1 T_g (T_g of PNC). We chose this temperature because it is the closest temperature to T_g where the interfacial layer relaxation process is still within the experimental frequency window of BDS. Interestingly, stronger slowing down of the interfacial dynamics is obtained for the lower molecular weight, and then it decreases monotonously. The interfacial dynamics for PNC-9k is seven times slower comparing to the neat polymer, while it is only five times slower in PNC-404k. Such results agree with our earlier results on MW dependence in PVAc/silica nanocomposites. [42] To verify that our results are not related to any non-equilibrium issues, we annealed the highest MW PNC (where we expect the longest equilibration times) at T_g + 50 K for an additional 15 days, which corresponds to about 10^{12} τ_α. Such an extremely long annealing did not produce any detectable changes in the segmental relaxation spectra (Fig. S5), indicating that the samples are either at equilibrium or are trapped in a very deep metastable state and are as close to equilibrium as experimentally possible. This was also confirmed by measuring spectra twice at two selected temperatures using different path-ways (see Materials and Methods section and details in SI). The spectra perfectly overlap demonstrating that our BDS results are independent of the cooling protocol. Finally, one may note that a strong

reduction of the physical aging rate has been reported in PNCs with attractive interactions at the interface. [58-59]

To evaluate the overall segmental dynamics in nanocomposites, the apparent peak maximum in the dielectric spectra is fitted with a single HN function over a restricted frequency range (Figure 4a), i.e., without any decomposition on interfacial layer and bulk contributions in this case. The corresponding time scales are included in Figure 5a. At high temperatures, the segmental relaxation times of the bulk polymer and the main PNC process tend to converge for both MWs. As the temperature approaches T_g (τ_α = 100 s), the slowing down of the main peak in the PNC relative to the pure matrix is stronger in PNC-9k than in PNC-404k. Such an observation indicates that the behavior of the T_g-shift strongly depends on the molecular weight in these PNCs. The dynamic glass-transition temperature can be determined by fitting the temperature dependence of the segmental relaxation times (main process for PNCs) to the Vogel-Fulcher-Tammann (VFT) equation (Figure 5a), and extrapolating to the temperature at which τ_α = 100 s. The obtained values are in good agreement with the calorimetric T_g (see Table 1 and Figure 5b). For the lowest molecular weight, the difference in T_g between the nanocomposite and the neat polymer is the highest (5.3 K by TMDSC), and this difference decreases with the increase of molecular weight. It reaches the value of only 1.4 K for MW = 404 kg/mol. This result further confirms that the dynamics of the interfacial layer process has a larger slowing down in low-MW PNCs comparing to high-MW ones.

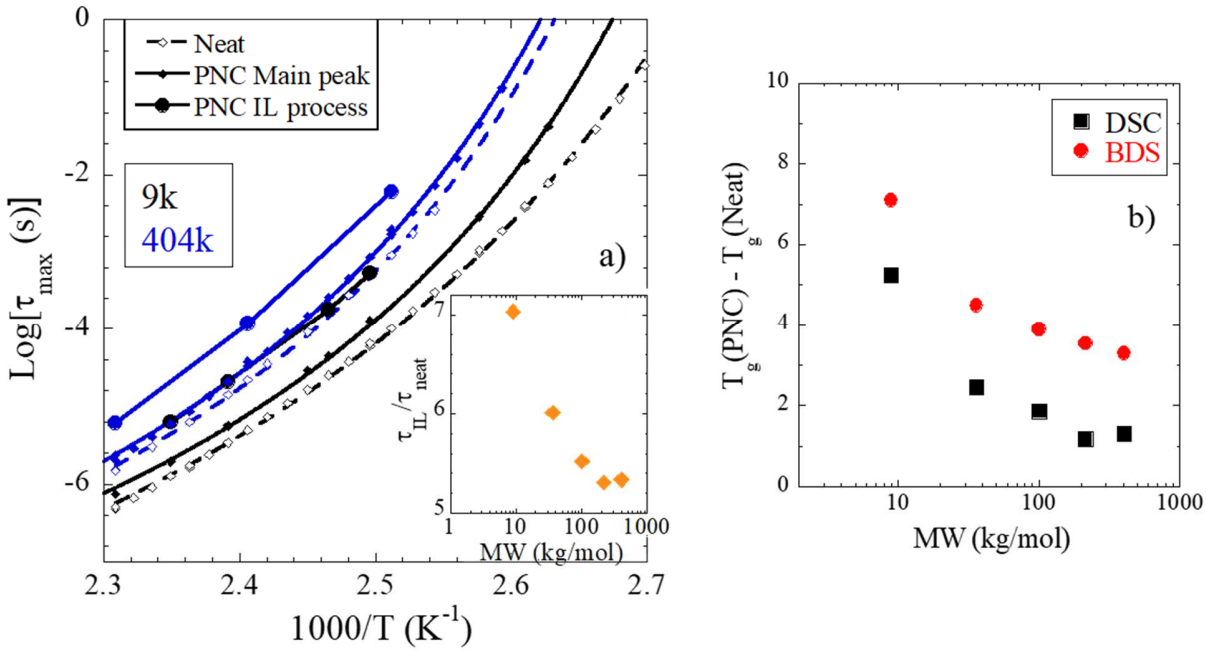

Figure 5. a) Temperature dependence of the interfacial segmental relaxation times, τ_{IL} (filled circles), for P2VP/silica nanocomposites with MW = 404 kg/mol (blue) and 9 kg/mol (black), averaged PNC dynamics (filled diamonds), and bulk-like dynamics, τ_{neat} (empty diamonds), with their fits by the Vogel-Fulcher-Tammann equation. Inset: Ratio of τ_{IL} to τ_{neat} corresponding to the interfacial layer slowing down at 1.1Tg. **b)** Change in T_g of PNCs with respect to corresponding neat polymers as a function of MW.

We now turn to the interfacial layer volume fraction, Φ_{IL}, obtained from the ILM analysis. One can see in Figure 6 that the interfacial layer fraction with slowed-down dynamics does not show any significant MW dependence, and takes an average value of 47 vol%. It means that there is only about 27 vol% of bulk-like polymer left in the interstitial space between nanoparticles, which gives rise to a bulk dielectric signal in all PNCs (another 26 vol% is occupied by silica). The estimation of the interfacial layer thickness from Φ_{IL} is straightforward using simple geometric considerations with a cubic arrangement of nanoparticles, and taking into account the overlapping volume between surrounding interfacial layers (see SI for details). We find an average thickness

of about 4.3 nm (Figure 6). It means that, in P2VP-silica PNCs, both the silica loading (see ref [52]) and MW do not play a significant role on the interfacial layer thickness.

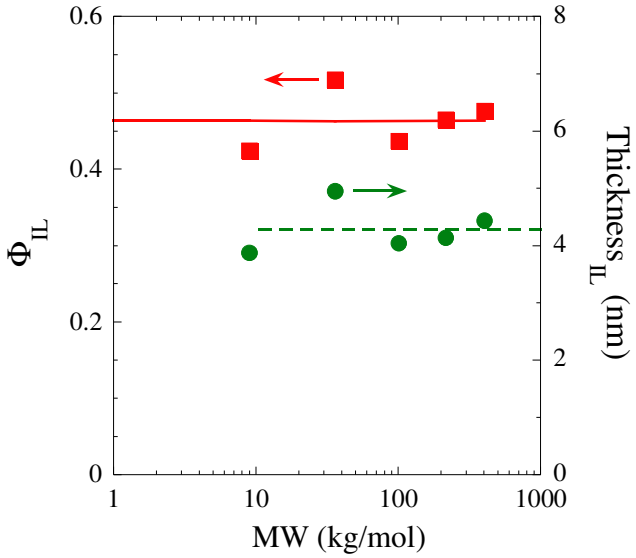

Figure 6. Volume fraction and estimated thickness of interfacial layer surrounding the silica nanoparticles in P2VP nanocomposites with similar loadings ($\Phi_{NP} \approx 26$ vol%) and different MWs. Lines show the average values.

Using the so obtained volume fraction, it is then possible to apply the ILM model and calculate the bulk and shear moduli of the interfacial layer from the BLS results (Table 1 and Figure 3). ILM predicts the elastic response of the nanocomposites as [36]

$$K_{PNC} = \frac{K_{NP}\,\Phi_{NP} + K_{IL}\,\Phi_{IL} R + K_{Neat}\,\Phi_{Neat} S}{\Phi_{NP} + \Phi_{IL} R + \Phi_{Neat} S} \quad (1)$$

with $S = \frac{(3K_{NP}+4G_{NP})(3K_{IL}+4G_{Neat}) - 12d(K_{IL}-K_{NP})(G_{IL}-G_{Neat})}{\Phi_{NP}+\Phi_{IL}R+\Phi_{Neat}S}$, $R = \frac{3K_{NP}+4G_{IL}}{3K_{IL}+4G_{IL}}$ and $d = \frac{\Phi_{NP}}{\Phi_{NP}+\Phi_{IL}}$.

$\Phi_{IL} + \Phi_{NP} + \Phi_{Neat} = 1$, where Φ is the volume fraction and the sub-indices Neat, NP, IL, and PNC stand for pure polymer (bulk), silica nanoparticles, interfacial layer, and nanocomposite, respectively. K_{IL} is the bulk modulus and G_{IL} the shear modulus of the interfacial layer. Further

details on the ILM calculation can be found in refs [10, 36]. In eq 1, the bulk and shear moduli of the nanoparticles are fixed to K_{NP} = 35.12 GPa and G_{NP} = 30.06 GPa, which are calculated by assuming the sound velocity of the NP is the same as in fused silica. [60] For all PNC samples, we use the average value of Φ_{IL} (47 vol%, see Figure 6), which was obtained at a selected temperature T = 1.1T_g (T_g of PNC) as the closest to the glassy state in our experiments. The mechanical properties of the interfacial layer calculated using eq 1 are presented in Figure 7a. The results reveal a significant increase in the glassy moduli of interfacial layer in the case of PNC-9k and PNC-36k, while a much weaker increase in shear modulus and even a drop in the bulk modulus are observed for the interfacial layer in PNC-216k and PNC-404k.

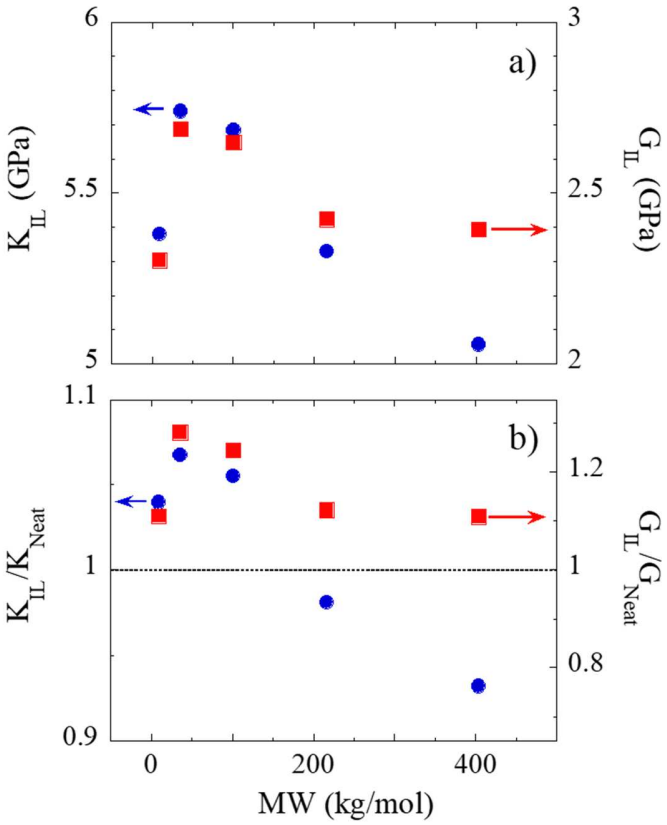

Figure 7. a) Bulk modulus, K_{IL}, and shear modulus, G_{IL}, of interfacial layer in P2VP/silica nanocomposites ($\Phi_{NP} \approx$ 26 vol%) from ILM calculations using Φ_{IL} = 47 vol%. **b)** Ratio of the mechanical moduli of interfacial layer to the moduli of the corresponding matrix (neat).

The differences observed between the interfacial layer moduli for PNCs with different molecular weights are likely the result of the difference in polymer rearrangement in the interface promoted by different MW of the matrix. Here, molecular features like chain packing, stretching of the polymer near the NP surface, [42] and polymer bridging play an important role. For instance, any difference in chain packing is expected to induce some changes in macroscopic density. To confirm this conjecture, we estimate the average density of the polymer matrix, ρ_{Matrix}^{PNC} , in the PNCs (Figure 8). The ratio of this quantity to the density of the neat polymer of same mass is shown in Figure 8a, where a clear evolution with molecular weight can be seen. The relative average density of the matrix in PNC is slightly higher than one for PNC-9k, as expected due to the attractive polymer-filler interaction, but then it decreases below one for higher molecular weights. This confirms that packing of the chains in nanocomposites depends strongly on the chain length. A similar evolution of $\rho_{matrix}^{PNC}/\rho_{Neat}$ with MW was reported and discussed in ref [42] for PVAc/silica PNCs, suggesting some general behavior of PNCs with attractive interactions.

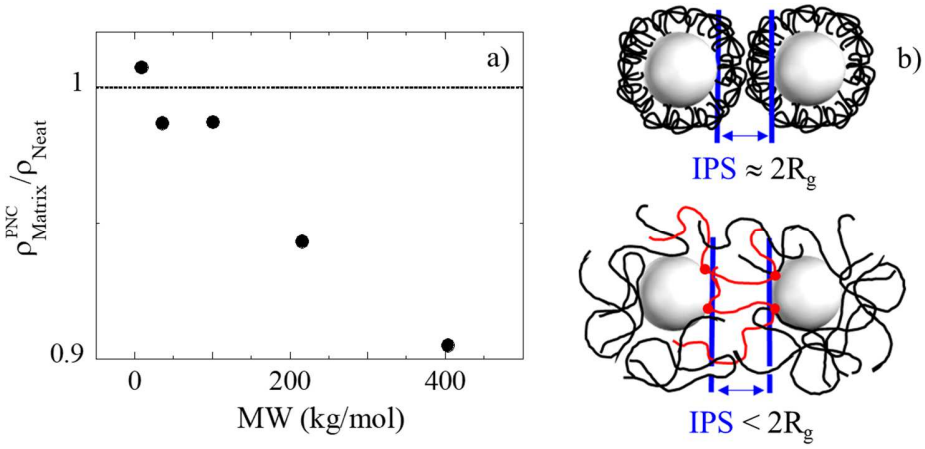

Figure 8. a) Ratio between average density of the matrix in P2VP/silica nanocomposite, ρ_{matrix}^{PNC} , and density of the pure polymer, ρ_{Neat}, for different molecular weights. $\rho_{matrix}^{PNC} = \frac{\rho_{PNC} - \rho_{NP}\Phi_{NP}}{1-\Phi_{NP}}$, where ρ_{PNC} and ρ_{NP} are the densities of PNC and silica NPs, respectively. **b)** Sketch of the chains confined between nanoparticles for low and high MW cases.

The density evolution can explain the decrease in mechanical properties of higher-MW PNCs, which is especially pronounced for PNC-216k and PNC-404k (Figure 7). The main idea here is that polymer chains adsorbed onto the silica NPs can experience different conformations, which are affected by many parameters, including MW and IPS. According to theory and simulations, adsorbed chains can form loops, trains, and tails near the NP surface. [40, 61] When the distance between NP surfaces becomes smaller than the size of the chain (~ 2 R_g), large polymer loops in high-MW PNCs are strongly confined between nanoparticles. [26, 42] This effect induces strong repulsive chain-chain interactions in the interfacial region, where the loops repel each other, leading to loose polymer packing and a lower density than in the bulk. However, in the case of low-MW PNCs, the chains are able to pack better because of their small size and the significant amount of free (non-adsorbed) chains. They may therefore arrange their conformation leading to a dense packing. This is in agreement with the evolution of the interfacial layer properties, which displays a stronger slowing down at low MW (inset of Figure 5a), while the volume fraction of interphase does not vary much (Figure 6). This behavior means that the dynamical changes observed in Figure 5 are not a function of how much polymer is impacted at the interface, but the result of different packing in the interfacial region. Since the density directly correlates with mechanical properties, the decrease in density ultimately leads to a decrease in mechanical moduli. However, density and chain packing alone are not sufficient to explain the maximum in bulk and shear moduli of interfacial layer obtained for PNC-36k. In this nanocomposite, the density is lower than the density of the pure polymer, while mechanical properties are maximal. Such behavior suggests the presence of other mechanisms of mechanical enhancement.

Bridging [62] of polymer chains between nanoparticles has been reported in literature for PNCs in glassy [10] and rubbery [8-9, 63] states. This mechanism is actively used in particle flocculation. [64] We believe that in our case, bridging is promoted by the high concentration of nanoparticles since the interparticle spacing is equal or smaller than 2 R_g of the polymer (Figure 1b). If polymer chains are adsorbed simultaneously on more than one particle, it can be expected that IPS displays a broader distribution, whereas absence of bridging may induce purely repulsive interactions leading to a narrower distribution of the interparticle distances. It is interesting to note that in PNC-9k, where the IPS is about 2 R_g of the polymer, the distribution of IPS deduced from the width of the repulsive interaction peak in SAXS is indeed narrower than in all other MWs (Figure 1a). This may suggest that bridging is unlikely for the low-MW PNC. The interaction peak becomes broader already in PNC-36k, and the most probable interparticle distance slightly decreases with increase of MW (IPS = 6.4 and 5.3 nm for MW = 36 and 404 kg/mol, respectively). This suggests initiation and possible progression of the bridges with decrease in IPS, as predicted by De Gennes for the case of flat surfaces.[9, 62] Chain bridging between nanoparticles, on one hand, leads to an improvement of the mechanical properties;[10] on the other hand, it facilitates a significant frustration in chain packing (see Figure 8b) that causes the drop in density and reduction of mechanical properties. Thus, the combined evolution of density and bridging may explain the non-monotonic behavior of mechanical properties with MW.

Another possible mechanism of mechanical enhancement is related to chain stretching in the interfacial layer. This effect has been proposed in theoretical works, [61, 65-66] where it was demonstrated that polymer adsorbed onto a solid wall will adopt a stretched conformation. It was also demonstrated experimentally for polymer brushes covalently grafted on a flat surface [67] or

grafted on spherical nanoparticles. [68-69] However, the degree of stretching for nanocomposites varies with the chain length. For instance, using self-consistent field theory calculations in PNCs, it was shown that stretching decreases with the MW increase. [70] Furthermore, it has also been shown that chain stretching leads to enhancement of mechanical properties (along the stretching direction). [71-72] In our case, this would mean that short and intermediate chains are stretched stronger than longer chains, which might be the reason for improvement in mechanical properties in these PNCs. Unfortunately, we do not have any experimental measure of chain stretching to support this idea, and it is difficult to evaluate whether stretching, bridging, or some other effects dominate the enhancement of mechanical properties. However, the presented experimental results revealed the existence of optimal conditions for achieving mechanical reinforcement that are realized in PNC-36k in our case.

Although we do not have any direct evidence of chain stretching and bridging in PNCs (more theoretical and experimental studies are on the way to address these points), some indirect evidence exists in our studies. We found that the interfacial layer bulk modulus and shear modulus have a different behavior. The interfacial layer modulus G_{IL} is always above the shear modulus of the neat polymers (Figure 7b), while the bulk modulus K_{IL} is below that of the neat polymer at high MW. In general, bulk modulus relates to the inverse of material's compressibility and is more sensitive to the density, while shear modulus is a deformation that is more sensitive to the anisotropic conformation of the polymer chains and hence more affected by chain stretching and bridging. Furthermore, we also found that the segmental dynamics of the interfacial layer are slower than the bulk segmental dynamics in all PNCs, but the observed slowing down is more pronounced at low MW. This finding is in line with theoretical works predicting a slowing down

of segmental dynamics [70, 73] in systems with more stretched polymer chains. Slowing down of the dynamics in our nanocomposites has a different magnitude with MW, further highlighting a complex interplay of chain stretching, packing (density), and bridging.

Conclusions

In summary, we presented measurements of mechanical properties in glassy P2VP/silica nanocomposites with different molecular weights and a single high NP loading (≈ 26 vol%). Our results suggest that mechanical properties are strongly influenced by the MW of the polymer and represent a complex interplay between chain packing, stretching, and bridging, which are acting in opposite directions. Strong enhancement in the glassy mechanical properties is achieved at low MW, with the maximum for PNC-36k, while further increase in MW results in a decrease of the mechanical properties enhancement. Such a non-monotonic dependence results from a complex interplay between chain packing and stretching in the interfacial polymer layer and formation of inter-particle bridges. Using ILM, and the independently estimated thickness of the interfacial layer, we estimated the glassy mechanical moduli in the interfacial region surrounding nanoparticles. The interfacial region occupies about 64 %vol of the polymer matrix in the studied PNCs. The mechanical moduli of the interfacial layer exhibit strong enhancement at low MW that decreases at larger MW due to frustration in packing of chains strongly confined between nanoparticles. In particular, the bulk modulus in the interfacial layer of high-MW PNCs appears to be even lower than in the neat polymer. Our results also reveal that the slowing down of PNC segmental dynamics and the shift in PNC T_g decrease with polymer MW, suggesting a common structural origin controlling glassy moduli and structural relaxation in nanocomposites. We

emphasize that the presented finding provides a clear guidance on how mechanical properties of glassy PNCs can be tuned by changing only polymer molecular weight.

Supporting Information: Normalization of BDS data, characterization results, BLS data of all materials tested, additional comparison of BDS spectra, annealing effect, estimation of the overlapping volume between interfacial layers,

Author Contributions: All authors contributed to writing the manuscript and have given approval to the final version of the manuscript.

ACKNOWLEDGMENT

This work was supported by the U.S. Department of Energy, Office of Science, Basic Energy Sciences, Materials Sciences and Engineering Division. ACG and JO are thankful for support by the ANR NANODYN project, Grant ANR-14-CE22-0001-01 of the French Agence Nationale de la Recherche. SAXS measurements by Philippe Dieudonné-George (L2C) are gratefully acknowledged.

ABBREVIATIONS

P2VP, Poly(2-vinyl pyridine); PNCs, polymer nanocomposites; MW, molecular weight; ILM, interfacial layer model; BDS, broadband dielectric spectroscopy; TMDSC, temperature-modulated differential scanning calorimetry; SAXS, small-angle X-ray scattering; BLS, Brillouin light scattering

REFERENCES

1. Suematsu, K.; Arimura, M.; Uchiyama, N.; Saita, S., Transparent $BaTiO_3$/PMMA Nanocomposite Films for Display Technologies: Facile Surface Modification Approach for $BaTiO_3$ Nanoparticles. *ACS Applied Nano Materials* **2018,** *1* (5), 2430-2437.
2. Mittal, V.; Kim, J. K.; Pal, K., *Recent Adances in Elastomeric Nanocomposites*. Springer-Verlag: Berlin Heidelberg, 2011.
3. Jancar, J.; Douglas, J. F.; Starr, F. W.; Kumar, S. K.; Cassagnau, P.; Lesser, A. J.; Sternstein, S. S.; Buehler, M. J., Current Issues in Research on Structure-Property Relationships in Polymer Nanocomposites. *Polymer* **2010,** *51* (15), 3321-3343.
4. Matteucci, S.; Kusuma, V. A.; Kelman, S. D.; Freeman, B. D., Gas Transport Properties of MgO Filled Poly(1-Trimethylsilyl-1-Propyne) Nanocomposites. *Polymer* **2008,** *49* (6), 1659-1675.
5. Chevigny, C.; Jouault, N.; Dalmas, F.; Boue, F.; Jestin, J., Tuning the Mechanical Properties in Model Nanocomposites: Influence of the Polymer-Filler Interfacial Interactions. *J. Polym. Sci., Part B: Polym. Phys.* **2011,** *49* (11), 781-791.
6. Mujtaba, A.; Keller, M.; Ilisch, S.; Radusch, H. J.; Beiner, M.; Thurn-Albrecht, T.; Saalwächter, K., Detection of Surface-Immobilized Components and Their Role in Viscoelastic Reinforcement of Rubber–Silica Nanocomposites. *ACS Macro Letters* **2014,** *3* (5), 481-485.
7. Berriot, J.; Montes, H.; Lequeux, F.; Long, D.; Sotta, P., Evidence for the Shift of the Glass Transition near the Particles in Silica-Filled Elastomers. *Macromolecules* **2002,** *35* (26), 9756-9762.

8. Papon, A.; Montes, H.; Lequeux, F.; Oberdisse, J.; Saalwächter, K.; Guy, L., Solid Particles in an Elastomer Matrix: Impact of Colloid Dispersion and Polymer Mobility Modification on the Mechanical Properties. *Soft Matter* **2012,** *8* (15), 4090-4096.
9. Chen, Q.; Gong, S.; Moll, J.; Zhao, D.; Kumar, S. K.; Colby, R. H., Mechanical Reinforcement of Polymer Nanocomposites from Percolation of a Nanoparticle Network. *ACS Macro Letters* **2015,** *4* (4), 398-402.
10. Cheng, S.; Bocharova, V.; Belianinov, A.; Xiong, S.; Kisliuk, A.; Somnath, S.; Holt, A. P.; Ovchinnikova, O. S.; Jesse, S.; Martin, H.; Etampawala, T.; Dadmun, M.; Sokolov, A. P., Unraveling the Mechanism of Nanoscale Mechanical Reinforcement in Glassy Polymer Nanocomposites. *Nano Letters* **2016,** *16* (6), 3630-3637.
11. Pryamitsyn, V.; Ganesan, V., Origins of Linear Viscoelastic Behavior of Polymer−Nanoparticle Composites. *Macromolecules* **2006,** *39* (2), 844-856.
12. Hashemi, A.; Jouault, N.; Williams, G. A.; Zhao, D.; Cheng, K. J.; Kysar, J. W.; Guan, Z.; Kumar, S. K., Enhanced Glassy State Mechanical Properties of Polymer Nanocomposites Via Supramolecular Interactions. *Nano Letters* **2015,** *15* (8), 5465-5471.
13. Kim, H.; Abdala, A. A.; Macosko, C. W., Graphene/Polymer Nanocomposites. *Macromolecules* **2010,** *43* (16), 6515-6530.
14. Su, S.; Jiang, D. D.; Wilkie, C. A., Methacrylate Modified Clays and Their Polystyrene and Poly(Methyl Methacrylate) Nanocomposites. *Polymers for Advanced Technologies* **2004,** *15* (5), 225-231.
15. Tao, R.; Simon, S. L., Bulk and Shear Rheology of Silica/Polystyrene Nanocomposite: Reinforcement and Dynamics. *J. Polym. Sci. B Polym. Phys.* **2015,** *53* (9), 621-632.

16. Smallwood, H. M., Limiting Law of the Reinforcement of Rubber. *J Appl Phys* **1944,** *15*, 758-766.

17. Guth, E., Theory of Filler Reinforcement. *J Appl Phys* **1945,** *16*, 20-25.

18. Einstein, A., Eine Neue Bestimmung Der Moleküldimensionen. *Annalen Der Physik* **1906,** *324* (2), 289-306.

19. Krishnamoorti, R.; Chatterjee, T., Carbon Nanotube-Based Poly(Ethylene Oxide) Nanocomposites. In *Handbook of Polymer Nanocomposites. Processing, Performance and Application: Volume B: Carbon Nanotube Based Polymer Composites*, Kar, K. K.; Pandey, J. K.; Rana, S., Eds. Springer Berlin Heidelberg: Berlin, Heidelberg, 2015; pp 299-334.

20. Akcora, P.; Kumar, S. K.; Moll, J.; Lewis, S.; Schadler, L. S.; Li, Y.; Benicewicz, B. C.; Sandy, A.; Narayanan, S.; Illavsky, J.; Thiyagarajan, P.; Colby, R. H.; Douglas, J. F., "Gel-Like" Mechanical Reinforcement in Polymer Nanocomposite Melts. *Macromolecules* **2010,** *43* (2), 1003-1010.

21. Oberdisse, J., Aggregation of Colloidal Nanoparticles in Polymer Matrices. *Soft Matter* **2006,** *2* (1), 29-36.

22. Baeza, G. P.; Genix, A. C.; Degrandcourt, C.; Petitjean, L.; Gummel, J.; Couty, M.; Oberdisse, J., Multiscale Filler Structure in Simplified Industrial Nanocomposite Silica/SBR Systems Studied by SAXS and TEM. *Macromolecules* **2013,** *46* (1), 317-329.

23. Akcora, P.; Liu, H.; Kumar, S. K.; Moll, J.; Li, Y.; Benicewicz, B. C.; Schadler, L. S.; Acehan, D.; Panagiotopoulos, A. Z.; Pryamitsyn, V.; Ganesan, V.; Ilavsky, J.; Thiyagarajan, P.; Colby, R. H.; Douglas, J. F., Anisotropic Self-Assembly of Spherical Polymer-Grafted Nanoparticles. *Nat Mater* **2009,** *8* (4), 354-359.

24. Maillard, D.; Kumar, S. K.; Fragneaud, B.; Kysar, J. W.; Rungta, A.; Benicewicz, B. C.; Deng, H.; Brinson, L. C.; Douglas, J. F., Mechanical Properties of Thin Glassy Polymer Films Filled with Spherical Polymer-Grafted Nanoparticles. *Nano Letters* **2012,** *12* (8), 3909-3914.

25. Kumar, S. K.; Jouault, N.; Benicewicz, B.; Neely, T., Nanocomposites with Polymer Grafted Nanoparticles. *Macromolecules* **2013,** *46* (9), 3199-3214.

26. Cheng, S.; Carroll, B.; Bocharova, V.; Carrillo, J.-M.; Sumpter, B. G.; Sokolov, A. P., Focus: Structure and Dynamics of the Interfacial Layer in Polymer Nanocomposites with Attractive Interactions. *J. Chem. Phys.* **2017,** *146* (20), 203201.

27. Berriot, J.; Montes, H.; Lequeux, F.; Long, D.; Sotta, P., Gradient of Glass Transition Temperature in Filled Elastomers. *Europhysics Letters* **2003,** *64* (1), 50-56.

28. Qu, M.; Deng, F.; Kalkhoran, S. M.; Gouldstone, A.; Robisson, A.; Van Vliet, K. J., Nanoscale Visualization and Multiscale Mechanical Implications of Bound Rubber Interphases in Rubber-Carbon Black Nanocomposites. *Soft Matter* **2011,** *7* (3), 1066-1077.

29. Cheng, X.; Putz, K. W.; Wood, C. D.; Brinson, L. C., Characterization of Local Elastic Modulus in Confined Polymer Films Via Afm Indentation. *Macromolecular Rapid Communications* **2015,** *36* (4), 391-397.

30. Xia, W.; Song, J.; Hsu, D. D.; Keten, S., Understanding the Interfacial Mechanical Response of Nanoscale Polymer Thin Films Via Nanoindentation. *Macromolecules* **2016,** *49* (10), 3810-3817.

31. VanLandingham, M. R.; Dagastine, R. R.; Eduljee, R. F.; McCullough, R. L.; Gillespie, J. W., Characterization of Nanoscale Property Variations in Polymer Composite Systems: 1. Experimental Results. *Composites Part A: Applied Science and Manufacturing* **1999,** *30* (1), 75-83.

32. Rouxel, D.; Thevenot, C.; Nguyen, V. S.; Vincent, B., Chapter 12 - Brillouin Spectroscopy of Polymer Nanocomposites. In *Spectroscopy of Polymer Nanocomposites*, William Andrew Publishing: 2016; pp 362-392.

33. Zhao, D.; Schneider, D.; Fytas, G.; Kumar, S. K., Controlling the Thermomechanical Behavior of Nanoparticle/Polymer Films. *ACS Nano* **2014,** *8* (8), 8163-8173.

34. Still, T.; Sainidou, R.; Retsch, M.; Jonas, U.; Spahn, P.; Hellmann, G. P.; Fytas, G., The "Music" of Core−Shell Spheres and Hollow Capsules: Influence of the Architecture on the Mechanical Properties at the Nanoscale. *Nano Letters* **2008,** *8* (10), 3194-3199.

35. Smith, J. C., Correction and Extension of Van der Poel's Method for Calculating the Shear Modulus of a Particulate Composite. *J. Res. Natl. Bur. Stand., Sect. A* **1974,** *78A* (3), 355-361.

36. Maurer, F. H. J. In *An Interlayer Model to Describe the Physical Properties of Particulate Composites*, Dordrecht, Springer Netherlands: Dordrecht, 1990; pp 491-504.

37. Maurice, G.; Rouxel, D.; Vincent, B.; Hadji, R.; Schmitt, J. F.; Taghite, M. b.; Rahouadj, R., Investigation of Elastic Constants of Polymer/Nanoparticles Composites Using the Brillouin Spectroscopy and the Mechanical Homogenization Modeling. *Polymer Engineering & Science* **2013,** *53* (7), 1502-1511.

38. Voudouris, P.; Choi, J.; Gomopoulos, N.; Sainidou, R.; Dong, H.; Matyjaszewski, K.; Bockstaller, M. R.; Fytas, G., Anisotropic Elasticity of Quasi-One-Component Polymer Nanocomposites. *ACS Nano* **2011,** *5* (7), 5746-5754.

39. Holt, A. P.; Bocharova, V.; Cheng, S.; Kisliuk, A. M.; Ehlers, G.; Mamontov, E.; Novikov, V. N.; Sokolov, A. P., Interplay between Local Dynamics and Mechanical Reinforcement in Glassy Polymer Nanocomposites. *Physical Review Materials* **2017,** *1* (6), 062601.

40. Scheutjens, J. M. H. M.; Fleer, G. J., Statistical Theory of the Adsorption of Interacting Chain Molecules. 2. Train, Loop, and Tail Size Distribution. *The Journal of Physical Chemistry* **1980,** *84* (2), 178-190.

41. Jouault, N.; Moll, J. F.; Meng, D.; Windsor, K.; Ramcharan, S.; Kearney, C.; Kumar, S. K., Bound Polymer Layer in Nanocomposites. *ACS Macro Letters* **2013,** *2* (5), 371-374.

42. Cheng, S. W.; Holt, A. P.; Wang, H. Q.; Fan, F.; Bocharova, V.; Martin, H.; Etampawala, T.; White, B. T.; Saito, T.; Kang, N. G.; Dadmun, M. D.; Mays, J. W.; Sokolov, A. P., Unexpected Molecular Weight Effect in Polymer Nanocomposites. *Physical Review Letters* **2016,** *116* (3).

43. Hidehiro, K.; Hisao, S.; Daisuke, K.; Genji, J., Densification of Alkoxide-Derived Fine Silica Powder Compact by Ultra-High-Pressure Cold Isostatic Pressing. *Journal of the American Ceramic Society* **1993,** *76* (1), 54-64.

44. Barrall, E. M.; Cantow, M. J. R.; Johnson, J. F., Variation of Refractive Index of Polystyrene with Molecular Weight: Effect on the Determination of Molecular Weight Distributions. *Journal of Applied Polymer Science* **1968,** *12* (6), 1373-1377.

45. Kremer, F.; Schönhals, A., *Broadband Dielectric Spectroscopy*. Springer-Verlag: Heidelberg, 2003.

46. Krüger, J. K.; Embs, J.; Brierley, J.; Jiménez, R. A., A New Brillouin Scattering Technique for the Investigation of Acoustic and Opto-Acoustic Properties: Application to Polymers. *Journal of Physics D: Applied Physics* **1998,** *31* (15), 1913.

47. Hao, T.; Riman, R. E., Calculation of Interparticle Spacing in Colloidal Systems. *J. Colloid Interface Sci.* **2006,** *297* (1), 374-377.

48. Meth, J. S.; Zane, S. G.; Chi, C.; Londono, J. D.; Wood, B. A.; Cotts, P.; Keating, M.; Guise, W.; Weigand, S., Development of Filler Structure in Colloidal Silica-Polymer Nanocomposites. *Macromolecules* **2011,** *44* (20), 8301-8313.

49. Jouault, N.; Zhao, D.; Kumar, S. K., Role of Casting Solvent on Nanoparticle Dispersion in Polymer Nanocomposites. *Macromolecules* **2014,** *47* (15), 5246-5255.

50. Griffin, P. J.; Bocharova, V.; Middleton, L. R.; Composto, R. J.; Clarke, N.; Schweizer, K. S.; Winey, K. I., Influence of the Bound Polymer Layer on Nanoparticle Diffusion in Polymer Melts. *ACS Macro Letters* **2016,** *5* (10), 1141-1145.

51. Landau, L. D.; Lifshitz, E. M., *Mechanics: Course of Theoretical Physics*. 3rd ed: Butterworth-Heinemann, 1976; Vol. 1.

52. Holt, A. P.; Griffin, P. J.; Bocharova, V.; Agapov, A. L.; Imel, A. E.; Dadmun, M. D.; Sangoro, J. R.; Sokolov, A. P., Dynamics at the Polymer/Nanoparticle Interface in Poly(2-Vinylpyridine)/Silica Nanocomposites. *Macromolecules* **2014,** *47* (5), 1837-1843.

53. Gong, S.; Chen, Q.; Moll, J. F.; Kumar, S. K.; Colby, R. H., Segmental Dynamics of Polymer Melts with Spherical Nanoparticles. *ACS Macro Letters* **2014,** *3* (8), 773-777.

54. Steeman, P. A. M.; Maurer, F. H. J., An Interlayer Model for the Complex Dielectric-Constant of Composites. *Colloid Polym. Sci.* **1990,** *268* (4), 315-325.

55. Carroll, B.; Cheng, S.; Sokolov, A. P., Analyzing the Interfacial Layer Properties in Polymer Nanocomposites by Broadband Dielectric Spectroscopy. *Macromolecules* **2017,** *50* (16), 6149-6163.

56. Füllbrandt, M.; Purohit, P. J.; Schönhals, A., Combined FTIR and Dielectric Investigation of Poly(Vinyl Acetate) Adsorbed on Silica Particles. *Macromolecules* **2013,** *46* (11), 4626-4632.

57. Havriliak, S.; Negami, S., A Complex Plane Representation of Dielectric and Mechanical Relaxation Processes in Some Polymers. *Polymer* **1967,** *8*, 161-210.

58. Rittigstein, P.; Torkelson, J. M., Polymer–Nanoparticle Interfacial Interactions in Polymer Nanocomposites: Confinement Effects on Glass Transition Temperature and Suppression of Physical Aging. *J. Polym. Sci., Part B: Polym. Phys.* **2006,** *44*, 2935-2943.

59. Cangialosi, D.; Boucher, V. M.; Alegría, A.; Colmenero, J., Physical Aging in Polymers and Polymer Nanocomposites: Recent Results and Open Questions. *Soft Matter* **2013,** *9* (36), 8619-8630.

60. Deschamps, T.; Margueritat, J.; Martinet, C.; Mermet, A.; Champagnon, B., Elastic Moduli of Permanently Densified Silica Glasses. *Scientific Reports* **2014,** *4*, 7193.

61. Guiselin, O., Irreversible Adsorption of a Concentrated Polymer Solution. *EPL (Europhysics Letters)* **1992,** *17* (3), 225.

62. de Gennes, P. G., Polymers at an Interface; a Simplified View. *Advances in Colloid and Interface Science* **1987,** *27* (3), 189-209.

63. Zhu, Z.; Thompson, T.; Wang, S.-Q.; von Meerwall, E. D.; Halasa, A., Investigating Linear and Nonlinear Viscoelastic Behavior Using Model Silica-Particle-Filled Polybutadiene. *Macromolecules* **2005,** *38* (21), 8816-8824.

64. Swenson, J.; Smalley, M. V.; Hatharasinghe, H. L. M., Mechanism and Strength of Polymer Bridging Flocculation. *Physical Review Letters* **1998,** *81* (26), 5840-5843.

65. Carrillo, J.-M. Y.; Cheng, S.; Kumar, R.; Goswami, M.; Sokolov, A. P.; Sumpter, B. G., Untangling the Effects of Chain Rigidity on the Structure and Dynamics of Strongly Adsorbed Polymer Melts. *Macromolecules* **2015,** *48* (12), 4207-4219.

66. Semenov, A. N.; Bonet-Avalos, J.; Johner, A.; Joanny, J. F., Adsorption of Polymer Solutions onto a Flat Surface. *Macromolecules* **1996,** *29* (6), 2179-2196.

67. Auroy, P.; Auvray, L.; Léger, L., Characterization of the Brush Regime for Grafted Polymer Layers at the Solid-Liquid Interface. *Physical Review Letters* **1991,** *66* (6), 719-722.

68. Schneider, D.; Schmitt, M.; Hui, C. M.; Sainidou, R.; Rembert, P.; Matyjaszewski, K.; Bockstaller, M. R.; Fytas, G., Role of Polymer Graft Architecture on the Acoustic Eigenmode Formation in Densely Polymer-Tethered Colloidal Particles. *ACS Macro Letters* **2014,** *3* (10), 1059-1063.

69. Hore, M. J. A.; Ford, J.; Ohno, K.; Composto, R. J.; Hammouda, B., Direct Measurements of Polymer Brush Conformation Using Small-Angle Neutron Scattering (SANS) from Highly Grafted Iron Oxide Nanoparticles in Homopolymer Melts. *Macromolecules* **2013,** *46* (23), 9341-9348.

70. Holt, A. P.; Bocharova, V.; Cheng, S.; Kisliuk, A. M.; White, B. T.; Saito, T.; Uhrig, D.; Mahalik, J. P.; Kumar, R.; Imel, A. E.; Etampawala, T.; Martin, H.; Sikes, N.; Sumpter, B. G.; Dadmun, M. D.; Sokolov, A. P., Controlling Interfacial Dynamics: Covalent Bonding Versus Physical Adsorption in Polymer Nanocomposites. *ACS Nano* **2016,** *10* (7), 6843-6852.

71. Wang, S.-Q.; Cheng, S.; Lin, P.; Li, X., A Phenomenological Molecular Model for Yielding and Brittle-Ductile Transition of Polymer Glasses. *The Journal of Chemical Physics* **2014,** *141* (9), 094905.

72. Zartman, G. D.; Cheng, S.; Li, X.; Lin, F.; Becker, M. L.; Wang, S.-Q., How Melt-Stretching Affects Mechanical Behavior of Polymer Glasses. *Macromolecules* **2012,** *45* (16), 6719-6732.

73. Oyerokun, F. T.; Schweizer, K. S., Theory of Glassy Dynamics in Conformationally Anisotropic Polymer Systems. *The Journal of Chemical Physics* **2005,** *123* (22), 224901.

TABLE OF CONTENTS